ACS Macro Letters

Letter

pubs.acs.org/macroletters

Tuning the Emission of Semiconducting Polymer Dots from Green to Near-Infrared by Alternating Donor Monomers and Their Applications for in Vivo Biological Imaging

Sz-Yu Liou,[†,§] Chi-Shiang Ke,[†,§] Jhih-Han Chen,[†] Yun-Wen Luo,[†] Shih-Yu Kuo,[†] You-Hong Chen,[†] Chia-Chia Fang,[†] Chang-Yi Wu,[‡] Chao-Ming Chiang,[†] and Yang-Hsiang Chan*[,†]

[†]Department of Chemistry and [‡]Department of Biological Sciences, National Sun Yat-sen University, 70 Lien Hai Road, Kaohsiung, Taiwan 80424

Supporting Information

ABSTRACT: Semiconducting polymer dots (Pdots) recently have emerged as a new class of extraordinarily bright fluorescent probes with promising applications in biological imaging and sensing. Herein multicolor semiconducting polymer nanoparticles (Pdots) were designed using benzothiadiazole (BT) as the acceptor, and various types of donors were incorporated to modulate their emission wavelengths. Specific cellular targeting and in vivo biotoxicity as well as microangiography imaging on zebrafish indicated these BT-based Pdots are promising candidates for biological applications.

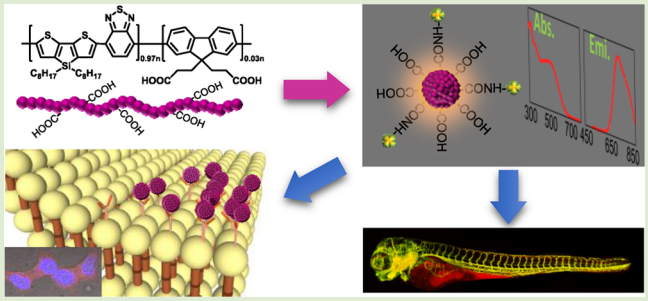

There have been great efforts made to explore biological processes in live organisms using fluorescent imaging techniques. Additionally, the new advances in fluorescence image-guided surgery have strongly emphasized the importance of using an appropriate fluorescent probe with high brightness, good photostability, low cytotoxicity, and high tumor specificity.[1,2] While conventional organic dyes often suffer from issues such as insufficient brightness and poor photostability, there have been several strategies developed to pursue brighter fluorescent agents. Among these fluorescent markers, nanoparticle-based fluorescent probes (e.g., dye-doped silica/polymeric nanocrystals or inorganic quantum dots)[3,4] exhibit much higher brightness and photostability. However, leakage of the embedded dyes from the silica matrix[5] and potential leaching of the toxic components (e.g., cadmium) from quantum dots[6] might impede their biological use and clinical implementation.

Semiconducting polymer nanoparticles (Pdots) have recently emerged as a new type of fluorescent probes with exceptional fluorescence brightness, excellent photostability, fast radiative rate, facile surface functionalization, and high biocompatibility.[7−14] Therefore, great efforts have been exerted to synthesize various types of Pdots emitting at different wavelengths,[15−21] and their sensing applications have been widely explored.[10,11,22−24] These π-conjugated copolymers usually based on donor−acceptor or donor−bridge−acceptor assemblies and efficient electron or energy transfer occur upon photoexcitation. Although several types of Pdots, especially in the near-infrared (NIR) range (700−1400 nm), have been extensively investigated, those Pdots often use fluorene (λ_{max}^{abs} < 400 nm) as the electron-rich segment (energy donor) whose excitation wavelength is less friendly for most biological applications.[16,17,20] Moreover, the information about the effect of donors on the optical properties (e.g., absorption, emission, and quantum yield) of Pdots is still lacking.

To address the aforementioned challenge and at the same time investigate the effect of the donor on the photophysical characteristics of Pdots, here we describe the design and synthesis of semiconducting polymers containing benzothiadiazole (BT) acceptors with different donors. More specifically, we systematically altered the donors on the conjugated polymer backbones (Scheme 1A) to obtain Pdots with tunable emission from green (ca. 550 nm) to NIR (ca. 760 nm). The resulting Pdots also exhibited distinct photophysical properties. We then directly tailored carboxyl functional groups on the side chains of the polymers and performed biomolecular conjugation for specific cellular labeling. Additionally, we conducted in vivo microangiography imaging on living zebrafish to demonstrate their promising potential in a broad range of biological studies and bioimaging.

Our aim was to synthesize BT-based Pdots with bright green to NIR emission by simply replacing the donor units. The general synthetic routes for the monomers and polymers were outlined in Scheme S1 (see Supporting Information). Their experimental details as well as characterization data (e.g., NMR, HRMS, etc.) were described in the Supporting Information. Briefly, various donors were first synthesized and then

Received: November 20, 2015
Accepted: December 3, 2015
Published: December 7, 2015

DOI: 10.1021/acsmacrolett.5b00842
ACS Macro Lett. 2016, 5, 154−157

Scheme 1. (A) Chemical Structures of a Series of BT-Containing Polymers, (B) Schematic Illustration of the Preparation of Carboxyl-Functionalized Pdots via Nanoprecipitation and Subsequent Bioconjugation for Specific Cellular Labeling and in Vivo Imaging, (C) Hydrodynamic Diameters of Si-PCPDBT-COOH Pdots (Average Diameter was 29 nm) Measured by Dynamic Light Scattering,[a] and (D) Photostability (Normalized Emission Intensity vs Time) of Si-PCPDBT Pdots (Black Curve), PFBT Pdots (Red Curve), and Cy5 Dyes (Blue Curve) In Bulk Aqueous Solutions (Except for Cy5 Dyes, Which Were in 1:20 DMSO/H_2O)

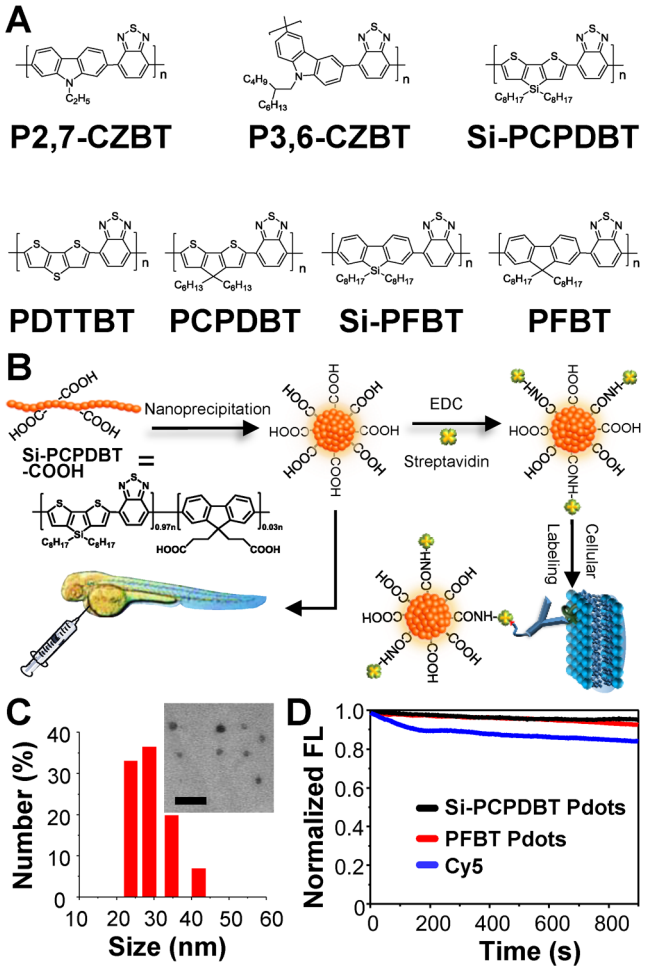

[a]The inset shows the transmission electron microscopy image of **Si-PCPDBT-COOH** Pdots. Scale bar is 50 nm.

polymerized with BT via Suzuki coupling. In an effort to provide functional groups for further bioconjugation (Scheme 1B), we fabricated carboxylate groups onto the side chains of fluorene moieties and then incorporated the carboxyl-functionalized fluorene into the polymer backbone. The resulting polymers were dissolved in THF and then nanoprecipitated in water under vigorous sonication to form carboxylic-acid-functionalized Pdots. The Pdots were subsequently conjugated to streptavidin via 1-ethyl-3-[3-(dimethylamino)propyl]-carbodiimide hydrochloride (EDC)-catalyzed coupling for specific cellular targeting and in vivo microangiography imaging on zebrafish. The average diameter of **Si-PCPDBT-COOH** Pdots determined by dynamic light scattering (DLS) was 29 nm (Scheme 1C). We also assessed the photostability of **PFBT** and **Si-PCPDBT** Pdots in comparison with Cy5 dyes. As shown in Scheme 1D, all of the three probes were photobleached under the same experimental conditions (380 nm excitation from a 150 W CW xenon lamp) at the same concentration of 200 pM. It can be seen that Pdots appeared to be extraordinarily photostable as compared to Cy5 dyes.

The absorption and emission spectra of seven types of BT-based Pdots are displayed in Figure 1. The upper panels in

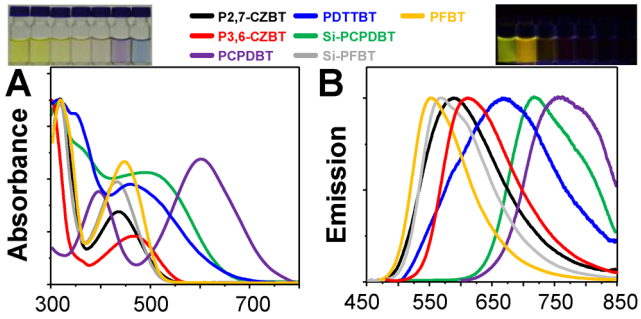

Figure 1. (A) UV−visible spectra of BT-based Pdot series in water. The upper panel shows the photograph of these Pdot solutions. (B) Fluorescence spectra of BT-based Pdot series in water. The upper panel shows the photograph of their corresponding Pdot solutions under UV (365 nm) illumination (from left to right: **PFBT**, **Si-PFBT**, **P2,7-CZBT**, **P3,6-CZBT**, **PDTTBT**, **Si-PCPDBT**, and **PCPDBT** Pdots in sequence). It should be noted that the light with wavelengths longer than 680 nm cannot be visualized by the naked eye.

Figure 1A and 1B represent the photographs of Pdot solutions under white light and 365 nm UV light, respectively (from left to right: **PFBT**, **Si-PFBT**, **P2,7-CZBT**, **P3,6-CZBT**, **PDTTBT**, **Si-PCPDBT**, and **PCPDBT** Pdots). It can be found the donors greatly affected both the absorption and emission properties of Pdots. Generally, the incorporation of the thiophene moiety or silicon atom could redshift both the absorption and the fluorescence peaks. The photophysical properties of these Pdot solutions were summarized in Table 1. **PCPDBT** Pdots have an

Table 1. Summary of Optical Properties of BT-Based Copolymer Series in Pdot Form in Water

copolymers	λ_{max}^{abs} (nm)[a]	λ_{max}^{em} (nm)[b]	size (nm)	Φ (%)[c]	fwhm[d]	τ (ns)[e]
PFBT	317, 446	550	26	23	98	0.75
Si-PFBT	316, 430	570	30	20	116	0.61
P2,7-CZBT	315, 434	587	29	2	145	1.01
P3,6-CZBT	468	612	29	3	129	0.43
PDTTBT	314, 459	674	28	1	195	0.44
Si-PCPDBT	314, 505	720	29	10	148	0.65
PCPDBT	395, 602	758	29	2	188	0.47

[a]Absorption maximum. [b]Fluorescence maximum. [c]Quantum yield. [d]Full width at half-maximum. [e]Fluorescence lifetime.

absorption peak at 602 nm and an emission maximum at 758 nm, which is excellent for in vitro and in vivo biological research due to the long penetration depth and minimal autofluorescence and scattering in tissues for NIR light. However, the quantum yield of **PCPDBT** Pdots is relatively low which might limit their practical use. On the other hand, **Si-PCPDBT** Pdots possess a good fluorescence quantum yield with NIR emission and could be readily excited by a commonly used 488 or 532 nm laser. These results indicate that the optical properties of the Pdots can be finely tuned by the modulation

DOI: 10.1021/acsmacrolett.5b00842
ACS Macro Lett. 2016, 5, 154−157

of different types of donors on the polymers. This information provides a very good background for further design of Pdots with different emission colors.

Moreover, we used a time-correlated single-photon counting module system to determine the fluorescence lifetime (τ) of this series of BT-based Pdots. The fluorescence radiative decay rate constant (K_R) and nonradiative rate constant (K_{NR}) containing all possible nonradiative decay pathways can also be estimated from the combination of the following two equations

$$\Phi = K_R/(K_R + K_{NR}) \quad (1)$$

$$\tau = (K_R + K_{NR})^{-1} \quad (2)$$

Take **Si-PCPDBT** Pdots as an example: the **Si-PCPDBT** Pdots have a fluorescence radiative decay rate of 1.5×10^8 S^{-1}, which is comparable to other types of Pdots.[18,25,26]

To demonstrate the applicability of these BT-based Pdots for biological imaging, we performed surface functionalization of Pdots by bioconjugating with streptavidin. Here we took Si-PCPDBT as an example owing to its good optical performance in the NIR range. Therefore, we first incorporated the carboxylated fluorene units into **Si-PCPDBT** polymer, that is, **Si-PCPDBT-COOH**. **Si-PCPDBT-COOH** Pdots were then used to label membrane proteins on MCF-7 breast cancer cells through the stable and specific streptavidin−biotin interaction. Specifically, **Si-PCPDBT-COOH** Pdots were conjugated with streptavidin via EDC-catalyzed coupling. The cells were incubated with biotinylated primary antihuman CD326 EpCAM antibody to target the EpCAM receptors. Subsequently, Pdot−streptavidin bioconjugates were introduced to label MCF-7 cells via the streptavidin−biotin interaction. Figure 2A reveals that the Pdot−streptavidin probes could be effectively labeled onto the surfaces of MCF-7 cells. On the contrary, a negligible fluorescence signal on the cell surface could be observed for the negative control (Figure 2B, in the absence of antibody), indicating minimal nonspecific adsorption occurred. For extensive biological applications and translation of these Pdots for widespread adoption, the cytotoxicity of Pdots is the major concern. We performed in vitro cytotoxicity experiments using an MTT assay and found no significant cytotoxic effect of these Pdots (500 pM) on HeLa cells (Figure 2C).

We also evaluated in vivo toxicity of Pdots by using zebrafish model. As shown in Figure 3A, we found that zebrafish could grow normally in the presence of Pdots (2−4 nM) even after 2 days. Both in vitro and in vivo results demonstrate that these Pdots exhibit high biocompatibility and are suitable for advanced biological implementation. Here we also carried out in vivo biological imaging in zebrafish because zebrafish possess several advantages over other vertebrate genetic systems.[27] For example, the optical transparency of zebrafish embryos and the capability of being genetically modified allow for direct observation of biological behaviors. Additionally, zebrafish models are evolutionarily close to human and can also be done in a large scale with very low cost, suitable for the experiments that require more variables and more robust statistics. For in vivo microangiography imaging on live zebrafish, we injected **Si-PCPDBT** Pdots into the sinus venous of the zebrafish larva. After injection, we found that the Pdots (red emission) were immediately distributed all over the vascular system and remained stable in the bloodstream without observation of leakage even 2 h after injection (Figure 3B(b)). The green fluorescence derived from eGFP-expressing

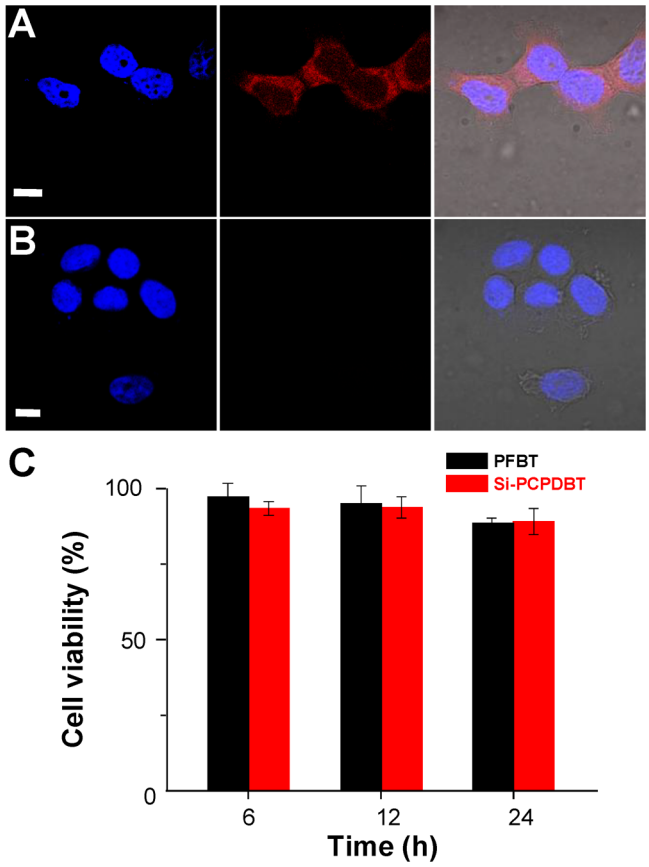

Figure 2. Two-color confocal fluorescence images of MCF-7 cells labeled with **Si-PCPDBT-COOH**−streptavidin conjugates. (A) Blue fluorescence is from nuclear counterstain Hoechst 34580, while red fluorescence is from Si-PCPDBT Pdots. The right panel represents fluorescence overlaid with the bright-field image. (B) Images of negative control samples in which MCF-7 cells were incubated with **Si-PCPDBT**−streptavidin probes but in the absence of primary biotin antihuman CD326 EpCAM antibody. The scale bars are 10 μm. (C) The impact of Pdots on cell viability determined by MTT assay.

endothelial cells could also be clearly seen in the blood vessel walls (Figure 3B(a)). Figure 3B(c) displays fluorescence overlaid of red and green fluorescence. Figure 3B(c,d) exhibits representative images of Pdot microangiography in zebrafish larvae, in which the prominent fluorescence signal from Pdots was revealed in the lumen of the vessels. However, some Pdots inevitably absorbed on the endothelial walls probably owing to the hydrophilicity of the Pdot surface. These results demonstrate that this type of BT-based Pdots has great biocompatibility and excellent fluorescence brightness, which is an ideal candidate for advancing in vivo biological studies.

In summary, we have successfully synthesized multicolor BT-containing fluorescent semiconducting copolymers by introducing different types of donors for energy transfer via Suzuki polymerization. The absorption and emission wavelengths of the corresponding Pdots could be thereby fine-tuned depending on the requirements of the instrument or experiments. The direct covalent functionalization of carboxylic acid groups on the side chains of the polymers offered the capability for further specific cellular targeting with minimal nonspecific adsorption. Moreover, we performed in vivo microangiography imaging on zebrafish larvae which showed the high stability and the sufficiently long circulation time of the Pdots in the bloodstream. We believe that this new class of multicolor

DOI: 10.1021/acsmacrolett.5b00842
ACS Macro Lett. 2016, 5, 154−157

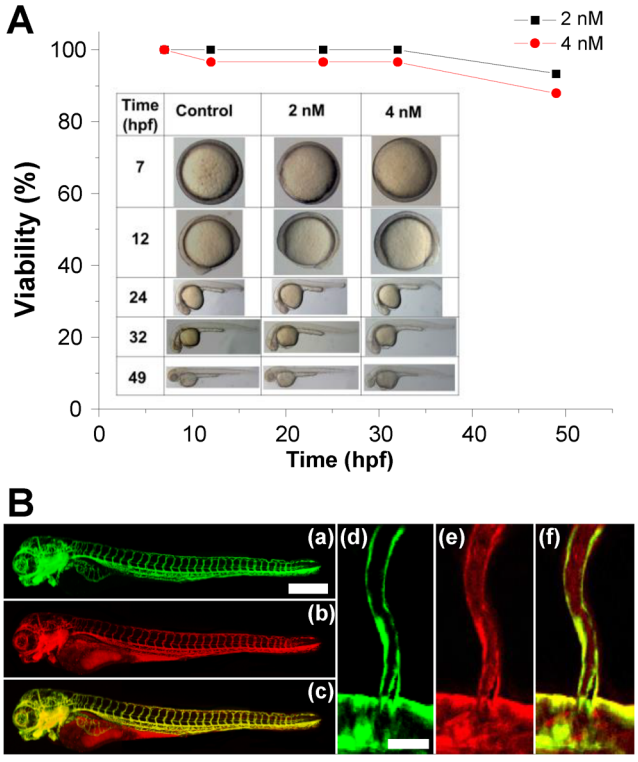

Figure 3. (A) Biotoxicity assessment of Pdots by the zebrafish model. Time course recording morphology of zebrafish embryos exposed to 2 and 4 nM Pdot solutions in the period of 0−49 h post fertilization (hpf). (B) Zebrafish microangiography by injection of **Si-PCPDBT-COOH** Pdots into 3 days post fertilization *Tg(kdrl:eGFP)* zebrafish embryos. The global view of zebrafish vessels is shown in left panels (a−c), while a close view of the trunk vasculature (intersegmental vessel, ISV) is shown in the right panels (d−f). Green emission is from endothelial cells expressing eGFP, and red emission is from Pdots. Scale bars represent 400 μm in (a) and 20 μm in (d), respectively.

BT-based Pdots can be widely adopted in both basic biological studies and bioanalytical detections.

■ ASSOCIATED CONTENT

Supporting Information

The Supporting Information is available free of charge on the ACS Publications website at DOI: 10.1021/acsmacrolett.5b00842.

Detailed synthetic procedures of BT-based copolymer series, experimental section, NMR spectra, cell culturing and labeling, and AFM images (PDF)

■ AUTHOR INFORMATION

Corresponding Author

*E-mail: yhchan@mail.nsysu.edu.tw.

Author Contributions

§These authors contributed equally to this work.

Notes

The authors declare no competing financial interest.

■ ACKNOWLEDGMENTS

We would like to thank the Ministry of Science (103-2113-M-110-004-MY2) and National Sun Yat-sen University. We also gratefully acknowledge support from Prof. Chao-Ming Chiang, Prof. Wei-Lung Tseng, Prof. Chin-Hsing Chou, and Dr. Jiun-Yi Shen from National Taiwan University.

■ REFERENCES

(1) Dam, G. M. v.; Themelis, G.; Crane, L. M. A.; Harlaar, N. J.; Pleijhuis, R. G.; Kelder, W.; Sarantopoulos, A.; Jong, J. S. d.; Arts, H. J. G.; Zee, A. G. J. v. d.; Bart, J.; Low, P. S.; Ntziachristos, V. *Nat. Med.* **2011**, *17*, 1315.
(2) Vahrmeijer, A. L.; Hutteman, M.; Vorst, J. R. v. d.; Velde, C. J. H. v. d.; Frangioni, J. V. *Nat. Rev. Clin. Oncol.* **2013**, *10*, 507.
(3) Bae, S. W.; Tan, W.; Hong, J.-I. *Chem. Commun.* **2012**, *48*, 2270.
(4) Michalet, X.; Pinaud, F. F.; Bentolila, L. A.; Tsay, J. M.; Doose, S.; Li, J. J.; Sundaresan, G.; Wu, A. M.; Gambhir, S. S.; Weiss, S. *Science* **2005**, *307*, 538.
(5) Peng, H.-s.; Stolwijk, J. A.; Sun, L.-N.; Wegener, J.; Wolfbeis, O. S. *Angew. Chem., Int. Ed.* **2010**, *49*, 4246.
(6) Tsoi, K. M.; Dai, Q.; Alman, B. A.; Chan, W. C. W. *Acc. Chem. Res.* **2013**, *46*, 662.
(7) Pecher, J.; Mecking, S. *Chem. Rev.* **2010**, *110*, 6260.
(8) Wu, C.; Chiu, D. T. *Angew. Chem., Int. Ed.* **2013**, *52*, 3086.
(9) Li, K.; Liu, B. *Chem. Soc. Rev.* **2014**, *43*, 6570.
(10) Kuo, S.-Y.; Li, H.-H.; Wu, P.-J.; Chen, C.-P.; Huang, Y.-C.; Chan, Y.-H. *Anal. Chem.* **2015**, *87*, 4765.
(11) Chan, Y.-H.; Jin, Y.; Wu, C.; Chiu, D. T. *Chem. Commun.* **2011**, *47*, 2820.
(12) Wu, C.; Schneider, T.; Zeigler, M.; Yu, J.; Schiro, P. G.; Burnham, D. R.; McNeill, J. D.; Chiu, D. T. *J. Am. Chem. Soc.* **2010**, *132*, 15410.
(13) Chan, Y.-H.; Wu, P.-J. *Part. Part. Syst. Charact.* **2015**, *32*, 11.
(14) Pu, K.; Shuhendler, A. J.; Jokerst, J. V.; Mei, J.; Gambhir, S. S.; Bao, Z.; Rao, J. *Nat. Nanotechnol.* **2013**, *9*, 233.
(15) Wu, P.-J.; Kuo, S.-Y.; Huang, Y.-C.; Chen, C.-P.; Chan, Y.-H. *Anal. Chem.* **2014**, *86*, 4831.
(16) Rong, Y.; Wu, C.; Yu, J.; Zhang, X.; Ye, F.; Zeigler, M.; Gallina, M. E.; Wu, I.-C.; Zhang, Y.; Chan, Y.-H.; Sun, W.; Uvdal, K.; Chiu, D. T. *ACS Nano* **2013**, *7*, 376.
(17) Wu, I.-C.; Yu, J.; Ye, F.; Rong, Y.; Gallina, M. E.; Fujimoto, B. S.; Zhang, Y.; Chan, Y.-H.; Sun, W.; Zhou, X.-H.; Wu, C.; Chiu, D. T. *J. Am. Chem. Soc.* **2015**, *137*, 173.
(18) Chen, C.-P.; Huang, Y.-C.; Liou, S.-Y.; Wu, P.-J.; Kuo, S.-Y.; Chan, Y.-H. *ACS Appl. Mater. Interfaces* **2014**, *6*, 21585.
(19) Geng, J.; Zhu, Z.; Qin, W.; Ma, L.; Hu, Y.; Gurzadyan, G. G.; Tang, B. Z.; Liu, B. *Nanoscale* **2014**, *6*, 939.
(20) Liu, H.-Y.; Wu, P.-J.; Kuo, S.-Y.; Chen, C.-P.; Chang, E.-H.; Wu, C.-Y.; Chan, Y.-H. *J. Am. Chem. Soc.* **2015**, *137*, 10420.
(21) Huber, J.; Jung, C.; Mecking, S. *Macromolecules* **2012**, *45*, 7799.
(22) Huang, Y.-C.; Chen, C.-P.; Wu, P.-J.; Kuo, S.-Y.; Chan, Y.-H. *J. Mater. Chem. B* **2014**, *2*, 6188.
(23) Chan, Y.-H.; Wu, C.; Ye, F.; Jin, Y.; Smith, P. B.; Chiu, D. T. *Anal. Chem.* **2011**, *83*, 1448.
(24) Ye, F.; Wu, C.; Jin, Y.; Chan, Y.-H.; Zhang, X.; Chiu, D. T. *J. Am. Chem. Soc.* **2011**, *133*, 8146.
(25) Chen, C.-P.; Wu, P.-J.; Liou, S.-Y.; Chan, Y.-H. *RSC Adv.* **2013**, *3*, 17507.
(26) Wu, C.; Bull, B.; Szymanski, C.; Christensen, K.; McNeill, J. *ACS Nano* **2008**, *2*, 2415.
(27) Lieschke, G. J.; Currie, P. D. *Nat. Rev. Genet.* **2007**, *8*, 353.

DOI: 10.1021/acsmacrolett.5b00842
ACS Macro Lett. 2016, 5, 154−157